

## Biofunctionalized pH-Responsive Microgels for Cancer Cell Targeting: Rational Design\*\*

By Mallika Das, Sawitri Mardiyani,  
Warren C. W. Chan,\* and Eugenia Kumacheva\*

Advancement in the design of polymer-based circulating drug-delivery systems (DDSs) has led to great improvements in the treatment of numerous diseases<sup>[1]</sup>. The major challenge in drug delivery is to maintain optimum therapeutic activity at target sites while minimizing adverse side effects. While macromolecular carriers (polymer chains and polymer-peptide conjugates) have shown much promise<sup>[2]</sup> as DDSs they have serious drawbacks, namely, weak protection of the drug from the body's defense mechanisms and potentially low drug-dose delivery to the target site. Particulate (or microreservoir) polymer-based DDSs, by contrast, provide a means of delivering drugs to diseased sites in high doses, thus protecting drugs from enzymatic degradation and preventing the delivery of drugs to healthy tissues.<sup>[3]</sup> Some of the useful particulate polymer-based DDSs include liposome-based or micelle-based DDSs.<sup>[4]</sup>

In this work we chose microgels as the particulate component of our DDS. Microgels have several important advantages over other particulate DDSs, namely, stability, ease of synthesis, good control over particle size, and easy functionalization providing stimulus-responsive behavior (e.g., change in volume in response to a change in pH, ionic strength, or temperature). Although Langer and co-workers<sup>[1a]</sup> and Frechet and co-workers<sup>[5]</sup> have reported pH-triggered non-specific release of a drug from microgels to the macrophages, the pH-responsive particles used in their experiments may be too large to reach tumor sites. Lyon and co-workers<sup>[6]</sup> reported folate-mediated cell targeting with microgels of diameter ca. 270 nm that exhibited temperature-dependent cytotoxicity.

However, cytotoxicity was only induced at 37 °C, which is too close to the temperature of healthy tissues. Very recently, Yang et al.<sup>[7]</sup> reported polymer core/shell microgels that were stable at pH 7.4 and 37 °C but deformed and precipitated in an acidic environment, triggering the release of the drug molecules. These particles however were not bioconjugated or tested in the cell environment. Baker and co-workers<sup>[8]</sup> have reported targeted cancer therapy using dendrimer-drug conjugates. The synthesis and purification of dendrimers is lengthy and cumbersome, and therefore less promising for practical applications.

Here we report a rational approach for cytosolic drug delivery to tumor cells based on the rational design of a microgel-based DDS. Our strategy was inspired by recent discoveries on characteristics of tumors,<sup>[9]</sup> which provide an excellent guide for the design of DDSs that selectively target diseased cells and release drugs only in specific biological conditions. We implemented the following criteria in the design of effective particulate DDSs for cancer therapy: 1) the presence of appropriate functional groups for conjugation with targeting species, which can selectively transport the microgels to a diseased site; 2) small (below 200 nm) size of microgels to maximize extravasation into tumors; 3) a release mechanism induced by biological stimuli such as a change in pH or interactions with enzymes, ions, or proteins; 4) incorporation of the drug into the microgel by physical means, as opposed to covalent attachment (which may potentially alter the drug's effectiveness).

We used pH-responsive microgels that possess all the aforementioned design requirements. The microgels were ca. 150 nm in size, close to a typical virus size under physiological conditions. We conjugated receptor-specific molecules onto the surface of the microgels for targeting diseased cells. Finally, an anticancer drug was loaded into the microgels by electrostatic interactions between the microgel and the drug. We demonstrated the feasibility of this microgel-based DDS to deliver small organic molecules and anticancer drugs into cancer cells by means of receptor-mediated endocytosis.

Poly(*N*-isopropylacrylamide acrylic acid), poly(NIPAM-AA) microgels were synthesized by means of free radical precipitation polymerization.<sup>[10]</sup> The molar ratio of the monomers [NIPAM]/[AA] in the reaction mixture was 9:1; the microgels were crosslinked with 4 mol-% *N,N'*-methylenebisacrylamide (BIS) and stabilized with 1 mol-% sodium dodecylsulphate (SDS). The average hydrodynamic diameter of the microgels after synthesis was ca. 150 nm, with a typical polydispersity of 0.1 (determined by photon correlation spectroscopy in 0.01 M phosphate-buffered saline at a pH of 7.4 and temperature of 37 °C). The lower critical solution temperature (LCST) of the copolymer microgels was well above the body temperature of 37 °C, due to the presence of the hydrophilic AA residues. At pH  $\approx$  7.4 the majority of the carboxylic groups of AA were ionized ( $\zeta$  potential of the microgel particles was  $-46$  mV), while at pH  $\approx$  4.5 they were largely protonated and carried only a weak charge ( $\zeta$  potential =  $-1.2$  mV). Figure 1a shows variation of microgel size in the range

[\*] Prof. E. Kumacheva, M. Das  
Department of Chemistry  
University of Toronto  
80 St George Street, Toronto  
Ontario, M5S 3H6 (Canada)  
E-mail: ekumache@chem.utoronto.ca

Prof. W. C. W. Chan, S. Mardiyani  
Institute of Biomaterials and Biomedical Engineering  
University of Toronto  
4 Taddlecreek Road, Toronto  
Ontario, M5S 3G9 (Canada)  
E-mail: warren.chan@utoronto.ca

[\*\*] E.K. thanks the Canada Research Chair for funding (NSERC Canada). W.C.W.C. acknowledges NSERC, CFI, OIT and the University of Toronto for financial support. M.D. thanks OGS for graduate fellowship. S.M. acknowledges NSERC for graduate fellowship.

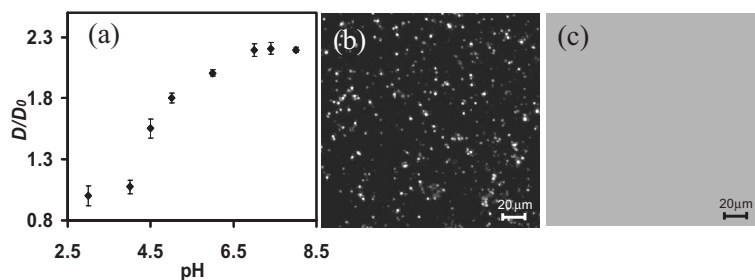


**Figure 1.** a) Variation of the size of the microgel particles as a function of pH. All measurements were taken at 25 °C in 0.01 M KCl. The average hydrodynamic diameter of the microgels was approximately 110 and 156 nm at pH 4.5 and 7.4, respectively. b,c) Optical fluorescence microscopy images of microgels loaded with R6G at pH 7.4 (b), and at pH 4.5 (c), examined under magnification.

$3.0 < \text{pH} < 8.0$ . At  $\text{pH} \approx 7.0$  the microgels were 50 % larger in size than at  $\text{pH} \approx 4.5$ . The increase in microgel size at  $\text{pH} \approx 7.0$  occurred due to osmotic swelling and electrostatic repulsion between the deprotonated COOH moieties, as well as the associated increase in hydrophilicity due to increased polarity of AA.<sup>[11]</sup>

The optical properties of Rhodamine 6G (R6G), a commercially available fluorescent dye carrying a positive charge, are relatively insensitive to pH changes.<sup>[12]</sup> R6G was introduced into the negatively charged microgel particles swollen in phosphate buffered saline (PBS) at pH 7.4. Figure 1b shows a typical optical microscopy image of the microgels loaded with R6G at pH 7.4. The presence of discrete bright spots on the dark background indicated that the dye was localized in the microgel particles. In contrast, at pH 4.5 a diffuse fluorescence signal in the background points to the release of R6G from the microgel interior into the continuous medium (Fig. 1c). The latter effect was attributed to microgel deswelling: protonation of the carboxylic groups resulted in suppression of both the repulsive electrostatic forces that caused swelling and the attractive electrostatic forces that maintained the dye within the microgel. Note that the optical microscopy image in Figure 1b was taken after the R6G-loaded microgels had been in buffered saline for 7 days. Although some non-triggered diffusion of R6G from the interior of microgels into the continuous medium could occur, Figure 1b indicates that at pH 7.4 electrostatic attraction between the microgels and R6G was sufficient to maintain a significant amount of dye within the microgel interior. Preliminary release profiles for microgels loaded with 35 % R6G (mg R6G/mg polymer) show that the cumulative release of R6G at pH 4.5 after 24 h was 88 % versus 12.5 % at pH 7.4. The values of pH used in these model release experiments were typical of those in the extracellular matrix (pH 7.4) and lysosome (pH 4.5) (final intracellular point of a molecule undergoing receptor-mediated endocytosis before entry into the cytoplasm).

In the next stage, we chose HeLa cancer cells to study the intracellular uptake of the pH-responsive, R6G-loaded microgel DDSs *in vitro*. HeLa cells have been extensively characterized for intracellular delivery through receptor-mediated

endocytosis, using the targeting, iron-carrying protein, transferrin.<sup>[13]</sup> The R6G-loaded microgels were conjugated to transferrin by carbodiimide coupling in PBS at pH 7.4 to utilize the presence of transferrin receptors on the surface of HeLa cells that enable endocytosis.<sup>[13]</sup> It should be noted that although carbodiimide coupling works best in the range of pH from 4.7 to 6.0, however it has been used effectively up to pH 7.5, without significant loss of yield.<sup>[14]</sup>

The targeting efficiency of the pH-responsive microgel DDSs was assessed with the aid of control experiments. Figure 2 shows differential interference contrast (left column) and corresponding epifluorescent images of HeLa cells (right column) after 24 h incubation with R6G-loaded microgels, not conjugated to any protein (Fig. 2a), conjugated to the non-endocytic protein, albumin (Fig. 2b), and conjugated to transferrin (Fig. 2c). A strong luminescence signal was ob-

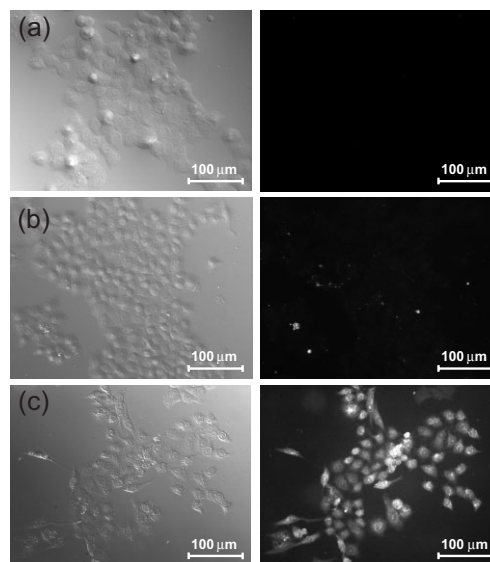


**Figure 2.** Differential interference contrast (DIC) (left) and epifluorescent (right) images of HeLa cells after 24 h incubation with R6G-loaded microgel-DDSs that were not conjugated to any protein (a), conjugated to albumin (b) and conjugated to transferrin (c). R6G is released from transferrin-conjugated microgels due to a change in pH during receptor-mediated endocytosis. 20× objective, numerical aperture NA=0.4,  $\lambda_{\text{ex}} = 480 \pm 40$  nm (100 W Hg lamp),  $\lambda_{\text{em}} = 535$  nm.

served only for HeLa cells incubated with transferrin-conjugated microgels (Fig. 2c) in contrast to the control systems (Fig. 2a,b) where only a weak luminescence was observed. A diffuse signal throughout the cells was observed when they were examined by high magnification (100×) fluorescence imaging, which suggests that R6G was delivered to the cytoplasm. No distinct patterns of subcellular staining indicating organellar location were observed. These observations confirmed that the release of R6G into the cytoplasm was due to

transferrin targeting of HeLa cells and pH-triggered deswelling of microgels upon exposure to the acidic lysosomal environment. We note that in these cell experiments, the microgels were incubated in media supplemented with fetal bovine serum, which contained proteins that may have interacted with the charged polymer. Our results show that the DDS was stable and effective in the presence of proteins in solution.

By measuring the luminescence intensity per cell we estimated that the transferrin-conjugated microgels delivered over 3 and 100 times more R6G to the cells than the albumin-conjugated and bare microgels, respectively. The slightly enhanced fluorescence observed for cells incubated with albumin-conjugated microgels (as compared to the bare microgels) was attributed to non-specific binding of albumin to HeLa cells.

We also examined the cytotoxicity of pH-responsive microgels loaded with Doxorubicin (Dox), a widely used anticancer drug. Dox is known to have side effects such as myelosuppression and cardiotoxicity; thus targeted delivery is especially advantageous for this drug.<sup>[15]</sup> At pH 7.4 Dox was positively charged, which assisted in electrostatically driven incorporation of Dox in the microgel interior. We compared the viability (percentage of cells surviving) of HeLa cells after 36 h incubation with transferrin-conjugated Dox-loaded microgels with that of several control systems. Cell viability was assessed using a Trypan Blue exclusion assay. Figure 3a shows that HeLa cells incubated with transferrin-conjugated Dox-loaded microgels had a viability of  $28.4 \pm 5.0\%$  (that is, a mortality of

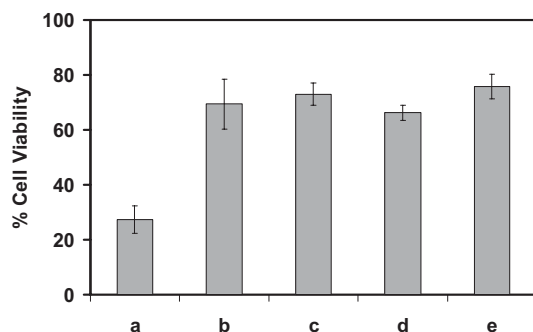


**Figure 3.** Viability of HeLa cells after incubation for 36 h in different systems: a) transferrin-conjugated Dox-loaded microgels; b) Dox-loaded microgels in solution with free transferrin (no conjugation); c) albumin-conjugated Dox-loaded microgels; d) plain Dox-loaded microgels (no conjugation); e) transferrin-conjugated plain microgels (in the absence of Dox).

$72.6 \pm 5.0\%$ ). The control systems included Dox-loaded microgels in solution with, but not conjugated to transferrin (Fig. 3b), albumin-conjugated Dox-loaded microgels (Fig. 3c), Dox-loaded non-conjugated microgels in buffer saline solution (Fig. 3d), and transferrin-conjugated microgels in the absence of Dox (Fig. 3e). These systems showed a cell mortality of  $30.6 \pm 9.1\%$ ,  $27 \pm 4.1\%$ ,  $33.8 \pm 2.8\%$ , and  $24.3 \pm 4.5\%$ , respectively. Thus, the mortality values of HeLa cells in all the

control systems were significantly lower than those for transferrin-conjugated Dox-loaded microgels, clearly indicating that biofunctionalized, pH-responsive microgels selectively carried the chemotherapeutic agent into tumor cells and caused significant cytotoxicity.

In summary, we demonstrated the rational design of a bioinspired DDS. Bioconjugated pH-responsive microgels offer a novel approach for highly specific targeting of cancer cells. We took advantage of the receptor-mediated endocytosis process and used pH changes in the intracellular environment for targeted delivery of organic molecules (including an anticancer drug) into the tumor cells. Although Dox and R6G are different organic molecules with different hydrophobicities and acid–base chemistry, our goal here was to show a proof-of-concept: that is, a pH-triggered approach for intracellular drug delivery by using appropriately tuned, pH-responsive copolymer microgels, biofunctionalized with a targeting ligand characteristic of the specific cancer cells being treated. In the near future, experiments will be extended to in-vivo systems and to biopolymer-based and biodegradable microgels.<sup>[16]</sup>

## Experimental

**Preparation of the Microgel:** *N*-isopropylacrylamide (NIPAM), acrylic acid (AA), *N,N*-methylenebis(acrylamide) (BIS), potassium persulfate (KPS), and sodium dodecyl sulfate (SDS) were purchased from Aldrich and used as received. Deionized water with a resistivity of 18.2 mΩ was used to make all solutions. Microgels with 9:1 mol-% ratio of NIPAM to AA were synthesized by means of free radical precipitation polymerization. All monomers, 4 mol-% BIS, and 1 mol-% SDS were dissolved in 80 ml of deionized water. The reaction mixture was heated to 65 °C under a steady stream of nitrogen in a three-necked round-bottom flask equipped with a condenser, an inlet for nitrogen, and a stirrer, for 1 h. 1.2 mol-% KPS was dissolved in 20 ml of deionized water and was then added to initiate the reaction. The reaction mixture was kept at 65 °C for 5 h to complete the reaction. The particles were then purified by dialysis with daily changes of water for 10 days (Spectra/Por, MWCO: 12–14,000).

**Particle Characterization:** Particle sizes were determined by photon correlation spectroscopy (PCS, Protein Solutions Inc.) equipped with a temperature controller. All solutions used for PCS measurements were diluted with deionized water and adjusted to the desired pH with HCl and/or NaOH while monitoring with an Ecomet pH meter. The hydrodynamic radii of the microgel particles were calculated from the translational diffusion coefficient using the Stokes–Einstein equation. For temperature measurements, the sample was allowed to equilibrate for 10 min at the desired temperature before data collection. The electrokinetic potential of the particles was measured using a Zetaser 3000 HS (Malvern Instruments).

**Trapping Rhodamine 6G in the Microgels:** 10 nmol of R6G was mixed with a 1 wt.-% microgel solution at pH 7.0. After incorporation in the microgel, excess R6G in the dispersion was removed by centrifugation. Optical microscopy images were taken after the dye-loaded gels had been in solution at pH 7.4 for at least 7 days. An estimate, based on fluorescence intensity measurements, shows that microgels, loaded with 35 % R6G (mg R6G/mg polymer) at pH 4 exhibit 88 % cumulative release after 24 h, versus 12.5 % shown by microgels in media of pH 7.4.

**Infusion of R6G and Dox into Microgels for Cell Studies:** 50 μL of the original microgel sample and 250 μL of  $10^{-4}$  M R6G was mixed together in 5 mL of PBS at pH 7.4 and allowed to equilibrate overnight.

This mixture was centrifuged at 12000 rpm and at 4 °C for 1 h. For Dox infusions, 500  $\mu\text{L}$  of  $3.68 \times 10^{-5}$  M Dox solution and 50  $\mu\text{L}$  of original microgel sample were incorporated in 5 mL of PBS (pH 7.4) before centrifugation. The Dox loading level of the microgels used in this study was 31.5 % (mg Dox/mg polymer).

**Bioconjugation of Transferrin to the Surface of Microgels:** The conjugation of transferrin and albumin to the microgels was accomplished by using the same process. A 10  $\text{mg mL}^{-1}$  stock solution of the proteins was made. 240  $\mu\text{L}$  of this solution was then mixed with 300  $\mu\text{L}$  of loaded gels in 0.01 M PBS at pH 7.4. Then, at least a 10-fold molar excess of 1-ethyl-3-(2-dimethylaminopropyl) carbodiimide hydrochloride was added to mediate the formation of an amide bond between carboxylic groups on the gel and amino groups on the protein.

**R6G-Loaded Microgel Assay:** HeLa cells were grown on cover slips in 100 mm tissue culture dishes until 50 % confluency was reached. R6G-loaded hydrogel particles, conjugated to transferrin, were dispersed in high glucose Dulbecco's modified eagle medium (DMEM) supplemented with 10 % fetal bovine serum, 1 % penicillin, and 1 % amphotericin B. For the controls, non-conjugated R6G-loaded microgel particles, particles conjugated to bovine serum albumin, and particles in solution with, but not conjugated to transferrin, were used. Cells were incubated overnight in this system. After washing the coverslips with 10 mM PBS, the cells were fixed with 3–4 % paraformaldehyde, followed by three washes with PBS. The cells were examined under 20 $\times$  magnification through differential interference contrast and epifluorescence. Quantitative analysis was based on the measurement of luminescence intensity per cell using ImagePro software.

**Dox-Loaded Microgels Assay:** One million HeLa cells were placed in each 60 mm tissue-culture dish and allowed to grow for two days. Dox-loaded hydrogel particles, conjugated to transferrin, were dispersed in high glucose DMEM, supplemented with 10 % fetal bovine serum, 1 % penicillin, and 1 % amphotericin B. HeLa cells were incubated for 36 h with Dox-loaded hydrogel particles conjugated to transferrin and control systems. The cells were then trypsinized, washed with PBS, and stained with Trypan Blue. The numbers of live and dead cells were counted under the microscope.

Received: May 21, 2005

Final Version: August 15, 2005

Published online: December 5, 2005

- [1] a) D. A. LaVan, D. M. Lynn, R. Langer, *Nat. Rev. Drug Discovery* **2001**, *1*, 77. b) M. A. Moses, H. Brem, R. Langer, *Cancer Cell* **2003**, *4*, 337.
- [2] A. K. Andrianov, L. G. Payne, *Adv. Drug Delivery Rev.* **1998**, *34*, 155.
- [3] S. S. Feng, G. Ruan, Q. Li, *Biomaterials* **2004**, *25*, 5181.
- [4] a) Y. Bae, S. Fukushima, A. Harada, K. Kataoka, *Angew. Chem. Int. Ed.* **2003**, *42*, 4640. b) R. Savić, L. Luo, A. Eisenberg, D. Maysinger, *Science* **2003**, *300*, 615. c) A. Eisenberg, D. Maysinger, *Science* **2004**, *303*, 627. d) M. F. Francis, M. Piredda, F. M. Winnik, *J. Controlled Release* **2003**, *93*, 59.
- [5] N. Murthy, M. Xu, S. Schuck, J. Kunisawa, N. Shastri, J. M. J. Frechet, *Proc. Natl. Acad. Sci.* **2003**, *100*, 4995.
- [6] S. Nayak, H. Lee, J. Chmielewski, L. A. Lyon, *J. Am. Chem. Soc.* **2004**, *126*, 10258.
- [7] K. S. Soppimath, D. Cherng-Wen Tan, Y. Yang, *Adv. Mater.* **2005**, *17*, 318.
- [8] A. K. Patri, A. Mycz, J. Beals, T. P. Thomas, N. H. Bander, J. Baker Jr., *Bioconj. Chem.* **2004**, *15*, 1174.
- [9] E. Ruoslahti, *Nat. Rev. Cancer* **2002**, *21*, 84.
- [10] H. N. Xiao, R. Pelton, A. Hamielec, *Polymer* **1996**, *37*, 1201.
- [11] a) B. R. Saunders, B. Vincent, *Adv. Colloid Interface Sci.* **1999**, *80*, 1. b) A. Fernandez-Nieves, A. Fernandez-Barbero, B. Vincent, F. J. De las Nieves, *J. Chem. Phys.* **2003**, *119*, 10383.
- [12] Y. Chen, J. D. Muller, K. M. Berland, E. Gratton, *Methods* **1999**, *19*, 234.
- [13] W. C. Chan, S. Nie, *Science* **1998**, *281*, 2016.

- [14] G. T. Hermanson, *Bioconjugate Techniques*, Academic Press, San Diego, CA **1996**.
- [15] N. K. Ibrahim, D. K. Frye, A. U. Buzdar, R. S. Walters, G. N. Hortobagyi, *Arch. Intern. Med.* **1996**, *156*, 882.
- [16] H. Zhang, M. Oh, C. Allen, E. Kumacheva, *Biomacromolecules* **2004**, *5*, 2461.

DOI: 10.1002/adma.200501033

## Fracture Transitions at a Carbon-Nanotube/Polymer Interface\*\*

By Asa H. Barber, Sidney R. Cohen, Ami Eitan, Linda S. Schadler, and H. Daniel Wagner\*

Carbon nanotubes represent a unique class of material where the mechanical properties of individual tubes are close to theoretically calculated values. The high strength<sup>[1–3]</sup> and stiffness<sup>[4–6]</sup> of carbon nanotubes are in excess of other fibrous materials and make them attractive as a structural material in future polymer composites. Critically, this reinforcement is effective only when the interfacial adhesion between the nanotube and surrounding polymer is substantial. We report in this work how the interfacial strength between a single carbon nanotube and a polymer matrix increases dramatically when the nanotube surface is chemically modified. This is shown by measuring the force required to pull individual nanotubes out of a polymer matrix using various embedded lengths. As opposed to our previous work,<sup>[7–9]</sup> the nanomechanical test is performed here in an electron microscope, which reveals a transition from nanotube pullout to fracture as the embedded length increases. This approach is powerful enough to elucidate the stress profile at an individual nanotube/poly-

[\*] Prof. H. D. Wagner, Dr. A. H. Barber  
Department of Materials and Interfaces  
Weizmann Institute of Science  
Rehovot 76100 (Israel)  
E-mail: daniel.wagner@weizmann.ac.il

Dr. S. R. Cohen  
Chemical Research Support  
Weizmann Institute of Science  
Rehovot 76100 (Israel)

Dr. A. Eitan, Prof. L. S. Schadler  
Department of Materials Science and Engineering  
Rensselaer Polytechnic Institute  
110 8<sup>th</sup> Street, Troy, NY 12180 (USA)

[\*\*] This project was supported by the (CNT) Thematic European network on "Carbon Nanotubes for Future Industrial Composites" (EU), the NOESIS European project on "Aerospace Nanotube Hybrid Composite Structures with Sensing and Actuating Capabilities", the Minerva Foundation, the G. M. J. Schmidt Minerva Centre of Supramolecular Architectures, and the Israeli Academy of Science. H. D. Wagner is the recipient of the Livio Norzi Professorial Chair.